7th International Conference on Innovation in
SCIENCE AND TECHNOLOGY
23 - 25 October, 2020 Amsterdam, Netherlands

Hybrid Vehicle Control based on road surface condition with Sliding Mode Control

Darioush Razmi [1], Mohammad Hossein kamaladini[2], Mohammad Hossein Modirrousta[3]
[1] Department of Electrical Engineering, Tabriz University, Tabriz, Iran
[2] Department of Electrical Engineering, Azaz University, Kerman, Iran
[3] Department of Electrical Engineering, K.N.Toosi University, Tehran, Iran

Abstract

The issue of stability control is one of the most important features of today's modern car. A control method was proposed to increase the stability of a hybrid vehicle with two independent motors on front and rear axle. This control method controls the torque of each wheel based on yaw rate, slip ratio, and lateral acceleration to prevent the vehicle deviation. Different structures are used for hybrid vehicle and the structure used in this article is a series one. To examine the performance of the proposed method, simulations were performed in MATLAB/SIMULINK software environment with Carsim software. The results of the simulations indicated that the proposed control method was capable of controlling the stability of the vehicle on slippery roads, so that it prevented the wheels from slipping and locking.

Keywords: Hybrid Vehicle, Stability Enhancement, Torque Control, Series Structure;

Introduction

Internal combustion vehicles are one of the biggest successes of modern technology. The number of cars around the world is growing and this has led to some serious environmental and hydrocarbon problems. Global warming, air pollution, and the depletion of oil resources are serious threats in today's world. Gradually, the threat of global warming and compliance with fuel efficiency standards have led vehicle manufacturers to take an important step in the automotive industry to improve and develop their products in terms of safety, cleanliness, and efficiency. Nowadays, this is proven to everyone that the technology of electric vehicles, electric hybrid, and fuel cell transmission systems can solve problems in the field of transport

for the future [1]-[2]. Different structures have been proposed for hybrid vehicles. One of which is a series structure. Due to its simple control strategy over other structures and also since the internal combustion engine operates at its highest efficiency, it can decrease fuel consumption and air pollution [3]. The issue of stability control, is one of the most important features of a modern car which includes maintaining the car's balance and proper track on road, especially in adverse conditions. The main cause of the car's instability is the inadequate torque distribution between wheels that if not done correctly, the driver may lose the control of the vehicle. By controlling the torque available for each wheel based on driver's need and condition of vehicle, it is possible to maintain stability and improve vehicle performance. Several research works have been done in this case such as vehicle dynamics control through controlling vehicle motion parameters such as yaw rate, lateral acceleration, and slip. Studies on vehicle dynamics control have investigated the effect of these parameters on improving vehicle stability, however, the interactions of these forces have not been seriously studied. The control method presented in this paper controls the torque of each wheel using its slip ratio, rotational speed, and lateral acceleration to prevent vehicle deviation. Given that rotational speed controller regulates the motion of the vehicle by distributing non-uniform longitudinal forces, the deformation of these forces at different friction coefficients is not negligible. Therefore, in this paper, the wheel slip controller is designed in a way that it can adapt to different road conditions and maintain its optimum performance at any given time [4, 5].

2. Hybrid Electric Drive Trains

As brief definition, a hybrid vehicle runs by connecting the elements that dictate the energy flow routes and control ports. Based on an old classification, HEVs have two types: series and parallel. It is notable that HEVs introduced after 2000 may not fit in this classification. Thus, four classes of HEVs were intoduced namely series hybrid, parallel hybrid, series–parallel hybrid, and complex hybrid. Fig.1 illustrates a fuel tank-IC engine and a battery-electric motor as representatives of the primary power source (steady power source) and secondary power source (dynamic power source) respectively. Clearly, different types of IC engines can be used as power source, such as fuel cells. In the same way, it is possible to replace the batteries by ultra-capacitors.

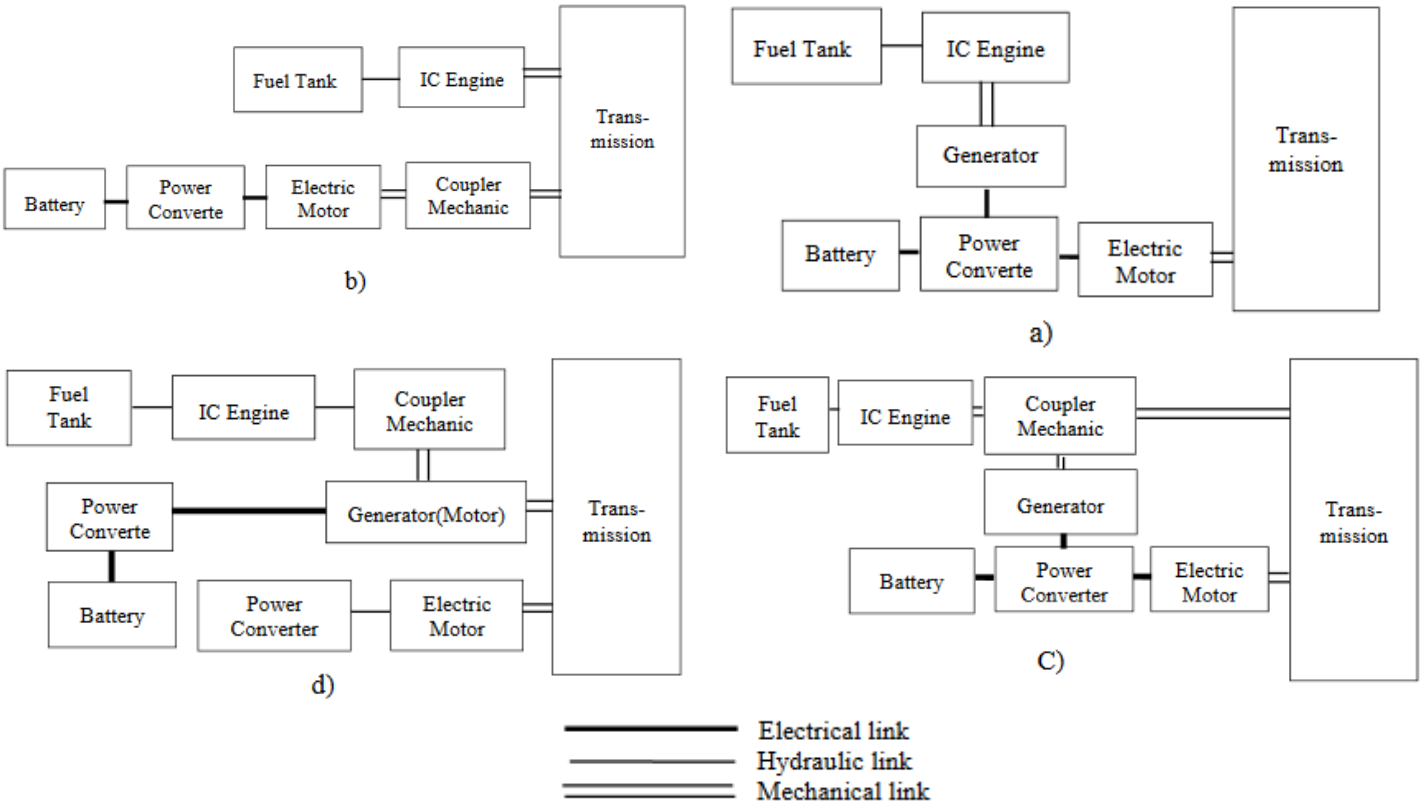

Fig.1: Hybrid Vehicle configuration, a) Series b) Parallel c) Series-Parallel d) Complex [1].

3. PROPOSED CONTROL ALGORITHM

Lateral acceleration, slip ratio, and yaw rate are the factors affecting vehicle dynamic motion. A torque control algorithm according to Fig.2 is presented for each wheel including tire slip controller, yaw rate controller, and lateral acceleration controller to avoid vehicle overturning in various road conditions, especially slippery roads.

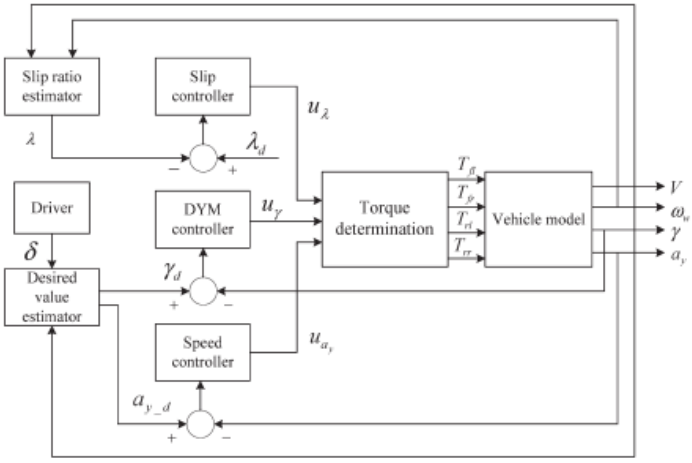

Fig. 2. Motor-torque control

3.1. Slip Ratio Controller

The slip controller, which is set up separately for each wheel, prevents locking or slipping of the wheels. For this purpose, the slip rate of each wheel must be maintained within the permissible range. Since the slip rate of 0.2% is defined as the boundary of the stable region (Fig. 4), the slip controller maintains λ in this range.

$$\lambda = \frac{r_t\omega - V}{r_t\omega} \quad driving \tag{1}$$

$$\lambda = \frac{V - r_t\omega}{r_t\omega} \quad braking \tag{2}$$

Where ω stands for the wheel rotational speed, r_t represents the wheel radius, and V refers to the vehicle velocity. Sliding surface σ can be given as follows

$$\sigma = me_\lambda + \dot{e}_\lambda \tag{3}$$

Where $\dot{e}_\lambda$ refers to the rate of e_λ, de_λ / dt and e_λ refers to the error between the target slip ratio λ_d and the actual slip ratio λ, e_λ is defined as

$$e_\lambda = \lambda_d - \lambda \tag{4}$$

Figure 3 illustrates a friction coefficient μ that has the same characteristics for different road conditions, so that as λ increases, it increases to some point and then it decreases. With a difference in absolute value, there is still a maximum friction coefficient in the range of λ = 0.15 ~ 0.2 on all types of road. Thus, the slip ratio ranges between λ = 0.15 and 0.2.

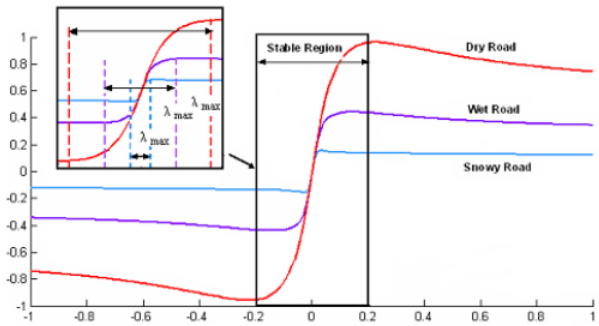

Fig.3. μ-λ curve for various road condition

Depending on the sliding surface, the control input is obtained

$$u_\lambda = \begin{cases} 1 & sign(\sigma) > 0 \\ u_{low_band} & sign(\sigma) < 0 \end{cases} \quad (5)$$

Where u_{low} bound refers to the low bound control gain and u_λ refers to sliding-mode control gain. To prevent high-frequency chattering, the sliding-mode control gain u_λ can be transmitted to the low-pass filter. The filtered control input "$u_{\lambda_{filter}}$" is as follows:

$$\tau_\lambda u_{\lambda_{filter}} + u_{\lambda_{filter}} = u_\lambda \quad (6)$$

Where τ_λ refers to the time constant of the low-pass filter. The $u_{\lambda_{filter}}$ controls the motor torque to make sure that the target slip ratio is achieved.

3.2. Yaw Rate Controller

The purpose of the yaw rate controller is to reduce the error between the vehicle's yaw rate and the preferred value. This controller adjusts the yaw rate of the vehicle by producing corrective yaw torque through distributing driving-braking forces on the wheels. The desired yaw rate is obtained as follows:

$$\gamma_d = \frac{V_x}{\left(L_f + L_r\right) + \left(\frac{W_f}{C_f} - \frac{W_r}{C_r}\right)\frac{V_x^2}{g}}\delta \tag{7}$$

Where *Vx* refers to longitudinal vehicle velocity, *Wf* refers to the normal load on each of the front tires, *Wr* stands for the normal load on each of the rear tires, *Cf* and *Cr* refer to the cornering stiffness of each of the front and rear tires respectively, and g refers to acceleration due to gravity.

Vehicle can move in lateral, longitudinal, and yaw directions (see Fig. 4), as follows:

$$I_z\dot{\gamma} = \sum M_z = M_{yaw} + M_{tire} \tag{8}$$

$$M_{yaw} = (F_{xfl} - F_{xfr})\cos\delta.\frac{\omega}{2} + (F_{xfl} + F_{xfr})\sin\delta.L_f + (F_{xrl} - F_{xrr}).\frac{\omega}{2} \tag{9}$$

$$M_{tire} = (F_{yfl} + F_{yfr})\cos\delta.L_f - (F_{yfl} - F_{yfr})\sin\delta.\frac{\omega}{2} - (F_{yrl} + F_{yrr}).L_r \tag{10}$$

Where γ stands for the yaw rate; Iz refers to the moment of inertia; *Mz* is the moment; *M*tire refers to the lateral tire moment. The lateral tire force by the tire depending on the stiffness of each wheel create the lateral tire moment; *M*yaw stands for the direct yaw moment caused by the longitudinal force at each wheel; *Lf* refers to the longitudinal distance from the center of gravity to the front tires; δ refers to the steering wheel angle; F stands for the force; *Lr* stands for the longitudinal distance between the center of gravity and the rear tires; subscripts x, y, and z stand for the longitudinal, lateral, and vertical directions respectively; w refers to the track width; fr indicates the front right wheel; rr indicates the rear right wheel; fl refers to the front left wheel; and rl stands for the rear left wheel.

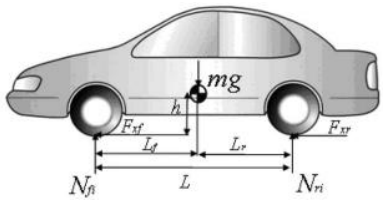

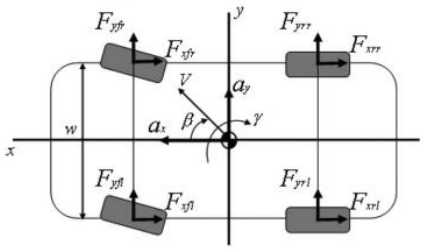

Fig. 4. Vehicle motion and parameters.

3.3. Lateral Acceleration

When the lateral acceleration exceeds the limit value sustainable at the tire contact patch, the vehicle might slip in the lateral direction, which creates instability. The preferred lateral acceleration ay_d is as follows:

$$a_{y-d} = \frac{V_x / g}{(L_f + L_r) + (\frac{W_f}{C_f} - \frac{W_r}{C_r}) V_x^2 / g} \delta \tag{11}$$

Since *ay_d* is a function of the longitudinal vehicle velocity *Vx*; when the lateral acceleration of the current exceeds *ay_d*, *the* velocity of vehicle must be lowered using an independent motor control. The controller output uay of the lateral acceleration is:

$$e_{a_y} = a_{y_d} - a_y \tag{12}$$

$$u_{a_y} = \begin{cases} k_p e_{a_y} & 0 \le k_p e_{a_y} \le 1 \\ 0 & k_p e_{a_y} < 0 \\ 1 & k_p e_{a_y} > 1 \end{cases} \tag{13}$$

Where *Kp* is the proportional gain of the error.

4. Motor Torque Control

Based on the control output obtained from the sliding-mode control of yaw ratio, fuzzy control of the lateral acceleration, the slip ratio, and the motor torque at each wheel is obtained as follows:

$$T_{fl} = T_d(A_p).u_{a_y}.u_{\lambda_{filter}}(\lambda_{fl}) - u_{\gamma_{filter}} \tag{14}$$

$$T_{fr} = T_d(A_p).u_{a_y}.u_{\lambda_{filter}}(\lambda_{fr}) + u_{\gamma_{filter}} \tag{15}$$

$$T_{rl} = T_d(A_p).u_{a_y}.u_{\lambda_{filter}}(\lambda_{rl}) - u_{\gamma_{filter}} \tag{16}$$

$$T_{rr} = T_d(A_p).u_{a_y}.u_{\lambda_{filter}}(\lambda_{rr}) + u_{\gamma_{filter}} \quad (17)$$

where Ap stands for the accelerator pedal opening, T refers to the motor torque, fl stands for front left, subscript d refers to the desired value, fr is front right, rl is rear left, and rr refers to rear right.

4. Analysis and Simulation Results

For simulation, CARSIM was used as a complete vehicle model in combination with MATLAB/Simulink. The simulated vehicle parameters are listed in Table (1). For generating propulsion power, two induction motors are used on the front and rear axles. These motors are controlled by the indirect vector control method. The parameters of this motors are the same as shown in Table (2).

Table 1: Simulated vehicle parameters

Parameter	Lf(mm)	Lr(mm)	Lw(mm)	Hg(mm)	Mt(kg)	Roll Inertia(kgm2)	Pitch Inertia(kgm2)	Yaw Inertia(kgm2)	Rw(mm)
amount	1070	1780	1880	660	1653	1243	4331	4331	398

Table 2: Induction motor parameters

Parameter	Lm(H)	Lr(H)	Ls(H)	Rr(ohm)	Rs(ohm)	B	J(kg/m2)	Pole Pairs
amount	0.403	0.0412	0.0415	0.25	0.3	0.02	0.1	2

Table (3) coefficients are used to model the aerodynamic resistance in the vehicle.

Table 3: Aerodynamic Resistance Parameters

Parameter	Frontal area(m2)	ρ (kg/m3)	Cf,r
amount	1.8	1.2	30000

The performance of the vehicle is tested on a Slalom test path (shown in Fig. 5) on a road with the road friction coefficient of 0.2 (in the case of icy roads) and vehicle speed of Vx = 80 km/h. Figure (5) shows the steering angle in the common mode.

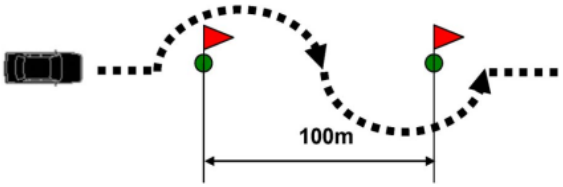

Fig.5. Slalom test path

When the vehicle arrives the corner in t=5s, the driver demands more steering angle, which is not suitable for following the desired path and leads to a deviation from the path (Fig.6). By applying the control strategy, according to Fig. (7), the requested steering angle corresponds to the path that leads to the corner in t=5s and following this path for 10 seconds, the vehicle enters the correct path in t=15s.

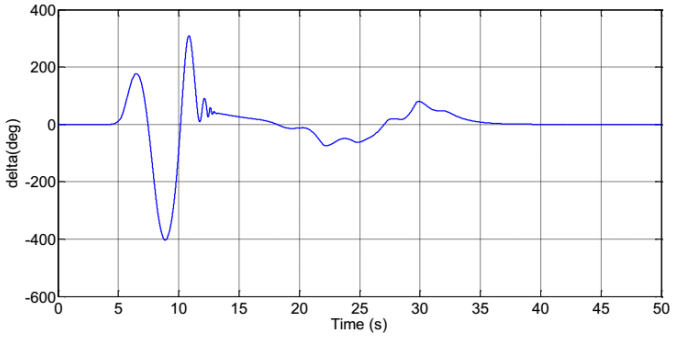

Fig. 6: steering changes in conventional mode.

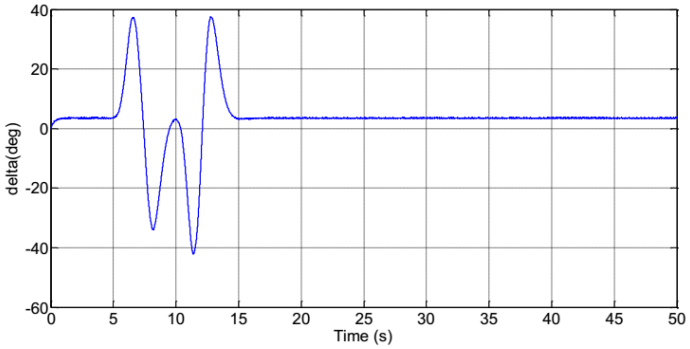

Fig. 7: steering changes with proposed strategy

To examine the performance of the proposed model, the results of wheel slip ratio were investigated. Figure 8&9 show the slip ratio of the wheels in conventional mode and control mode respectively. Clearly, in the conventional mode, when the vehicle arrives the corner, it slips and its slip ratio reach to -1. The vehicle slips in lateral directions and loses its stability. In control mode, on the corner, the slip value reaches -0.2 before the corner is over.

Afterwards, on a straight path, the slip value is close to zero, indicating a robust performance of the control system. It is notable that the slip value is negative when the vehicle decelerates and it is positive when the vehicle accelerates. Because the vertical load on each rear wheel is less than that on the front wheels, the friction force on the rear wheels is lower and the slip value also increases proportional to it.

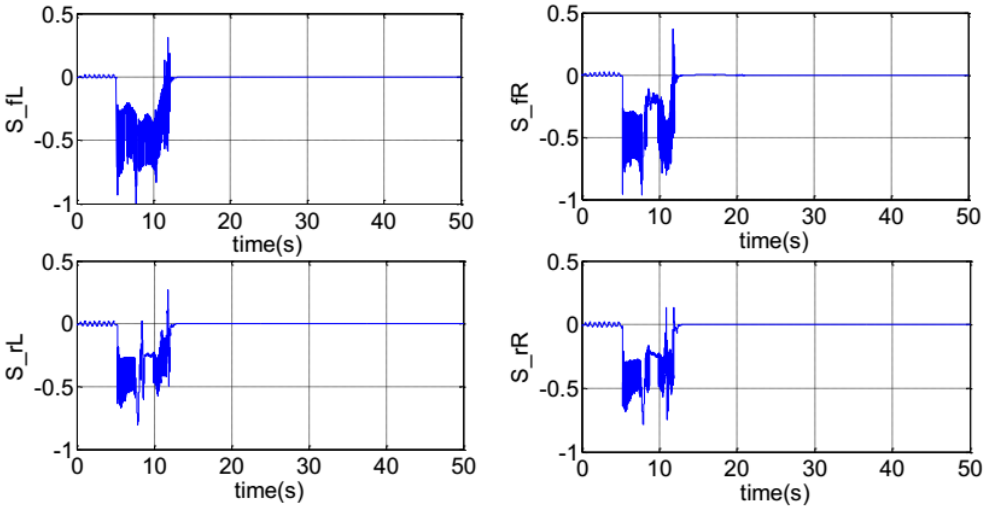

Fig. 8: Wheels slip ratio in conventional mode

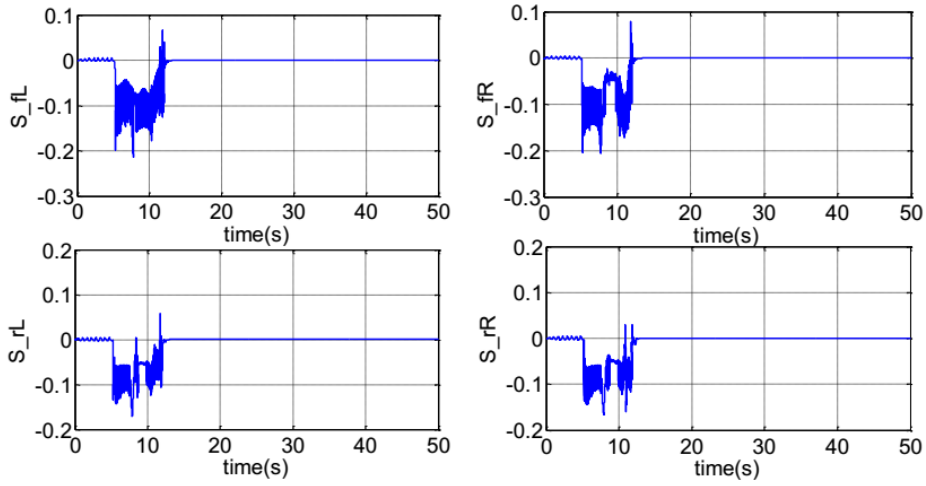

Fig. 9: Wheels slip ratio with proposed strategy

Figures 10&11 show the yaw rate of the vehicle in two conventional and control modes respectively. When the vehicle arrives the corner, the yaw rate increases appropriately and relative to the wheel steering angle. Clearly, the vehicle in conventional mode cannot have a better performance due to low friction coefficient so that it is diverted from the requested

path. In the controlled mode, the vehicle is properly controlled and remains stable. In the conventional mode, the yaw rate error is increased due to the increase of the steering angle over the corner. This throw the vehicle out of its balance state; while in control mode, this error is near zero – i.e. appropriate performance of the control system.

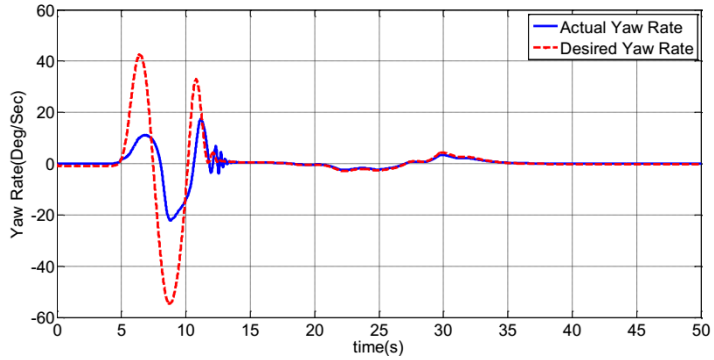

Fig. 10: Yaw rate wheel in conventional mode

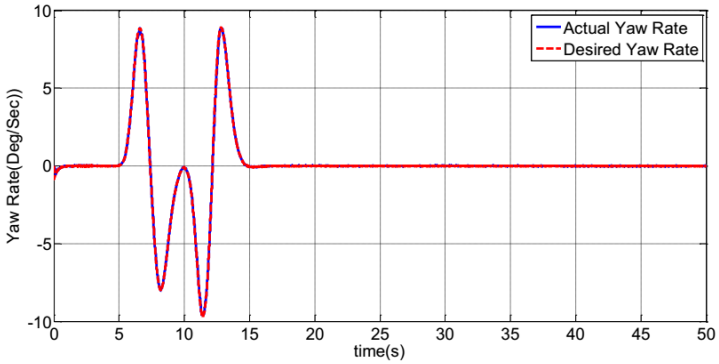

Fig. 11: Yaw rate wheel with proposed strategy

5. Conclusion

To increase the stability of the hybrid vehicle, a sliding mode control strategy was developed to prevent slippage on a slippery road. To examine the vehicle performance, the yaw rate and slip ratio of the wheels were set as stability criterion. It was shown that the vehicle lost its balance and slipped in conventional mode on all road conditions, while there was no slippage in the control mode. Using the control mode, the vehicle was able to adapt to road conditions and showed a successful test manoeuvre. The results supported the proper performance of the proposed system on slippery roads, so that it prevented slipping and locking.

References:

[1]	*C. Chuen Chan and K. Tim Chau. (2001), "Modern Electric Vehicle Technology, OxfordUniversity Press", New York, November.*
[2]	*M. Ehsani, Y. Gao and J. Miller. (2010),"Hybridelectric vehicles: Architecture andmotor drives", Proceedings of the IEEE, Special issue on Electric, Hybrid Electric and FuelCells Vehicle, Vol. 95, no. 4, April*
[3]	*K. Jiangmen, P. Chiman, S. Hwang and K. Hyunsoo. (2010), "Control Algorithm for an Independent Motor-Drive Vehicle", IEEE Transactions on vehicular Technology, Vol.59, no. 7, September.*
[4]	*Y. Hori, "Future vehicle driven by electricity and control-research on four-wheel-motored 'UOT electric march II,'" IEEE Trans. Ind. Electron. Vol. 51, no. 5, pp. 954–962, Oct. 2004.*
[5]	*B. Jacobsen, "Potential of electric wheel motors as new chassis actuators for vehicle maneuvering," Proc. Inst. Mech. Eng. Part D: J. Automobile Eng. vol. 216, no. 8, pp. 631–640, 2002*
[6]	K. Muta, M. Yamazaki and J. Tokieda, "Development of new-generation hybrid system THS II—Drastic improvement of power performance and fuel economy", *SAE World Congr*. 2004-March-811.
[7]	T. Horie, "Development aims of the new CIVIC hybrid and achieved performance", *Proc. SAE Hybrid Vehicle Technologies Symp*. 2006-Feb.12.
[8]	P. Struss and C. Price, "Model-based systems in the automotive industry", *AI Mag*. vol. 24, no. 4, pp. 17-34, 2004.
[9]	W. Gao, "Hybrid powertrain design using a domain-specific modeling environment", *Proc. IEEE Vehicle Power Propulsion Conf*. pp. 6-12, 2005-Sep.
[10]	K. B. Wipke, M. R. Cuddy and S. D. Burch, "ADVISOR 2.1: A user-friendly advanced powertrain simulation using a combined backward/forward approach", *IEEE Trans. Vehicular Technol*. vol. 48, no. 6, pp. 1751-1761, Nov. 1999.
[11]	T. Markel, A. Brooker, T. Hendricks, V. Johnson, K. Kelly, B. Kramer, et al. "ADVISOR: A systems analysis tool for advanced vehicle modeling", *J. Power Sources*, vol. 110, no. 2, pp. 255-266, Aug. 2002.
[12]	C. C. Lin, Z. Filipi, Y. Wang, L. Louca, H. Peng, D. Assanis, et al. "Integrated feed-forward hybrid electric vehicle simulation in Simulink and its use for power management studies", *Proc. SAE 2001 World Congr*. 2001-Mar.
[13]	K. L. Butler, M. Ehsani and P. Kamath, "A Matlab-based modeling and simulation package for electric and hybrid electric vehicle design", *IEEE Trans. Vehicular Technol*. vol. 48, no. 6, pp. 1770-1118, Nov. 1999.
[14]	X. He and J. W. Hodgeson, "Modeling and simulation for hybrid electric vehicles I. Modeling", *IEEE Trans. Intelligent Transportation Syst*. vol. 3, no. 4, pp. 235-243.
[15]	L. Gao, S. Liu and R. A. Dougal, "Dynamic lithium-ion battery model for system simulation", *IEEE Trans. Components Packaging Technol*. vol. 25, no. 3, pp. 495-505, Sep. 2002.
[16]	L. Gao, S. Liu and R. A. Dougal, "Active power sharing in hybrid battery/capacitor power sources", *Appl. Power Electronics Conf. Expo*. vol. 1, pp. 497-503, 2003.
[17]	K. Suzuki and S. Awazu, "Four-track vehicles by bond graph-dynamic characteristics of four-track vehicles in snow", *Proc. 26th Ann. Conf. IEEE Industrial Electronics Soc. IECON 2000*, vol. 3, pp. 1574-1579, 2000-Oct.
[18]	J.H. Kim and D. D. Cho, "An automatic transmission model for vehicle control", *Proc. IEEE Conf. Intelligent Transportation System ITSC 97*, pp. 759-764, 1997-Nov.
[19]	N. Nishijiri, N. Kawabata, T. Ishikawa and K. Tanaka, "Modeling of ventilation system for vehicle tunnels by means of bond graph", *Proc. 26th Ann. Conf. IEEE Industrial Electronics Soc. IECON 2000*, vol. 3, pp. 1544-1549, 2000-Oct.
[20]	G. A. Hubbard and K. Youcef-Toumi, "Modeling and simulation of a hybrid-electric vehicle drivetrain", *Proc. 1997 Amer. Contr. Conf*. vol. 1, pp. 636-640, 1997-Jun.46.